CSIRO Publishing

Publications of the Astronomical Society of Australia

VOLUME 18, 2001

An international journal of astronomy and astrophysics

For editorial enquiries and manuscripts, please contact:
The Editor, PASA,
ATNF, CSIRO,
PO Box 76,
Epping, NSW 1710, Australia
Telephone: +61 2 9372 4590
Fax: +61 2 9372 4310
Email: Michelle.Storey@atnf.csiro.au

For general enquiries and subscriptions, please contact:
CSIRO Publishing
PO Box 1139 (150 Oxford St)
Collingwood, Vic. 3066, Australia
Telephone: +61 3 9662 7666
Fax: +61 3 9662 7555
Email: pasa@publish.csiro.au

Published by CSIRO Publishing
for the Astronomical Society of Australia

www.publish.csiro.au/journals/pasa

Publ. Astron. Soc. Aust., 2001, 18, 345–350

Investigation of Coronal Mass Ejections I. Loop-type with Arcade Flare between the Fixed Legs, and Bubble-type Due to Flare Blast Waves

Y. Uchida, T. Tanaka, M. Hata and R. Cameron

Physics Department, Science University of Tokyo, Shinjuku-ku, Tokyo

Received 2001 July 13, accepted 2001 September 27

Abstract: In this paper, we give arguments that there are two types of coronal mass ejection (CME).

The first type of CME discussed here is the 'loop-type', whose occurrence is related to an arcade flare somewhere between the footpoints. It was found that there were pre-event magnetic connections between the flare location and the locations of the footpoints of a CME of this type, and that these connections disappeared after the event. This suggests that the footpoints of loop-type CMEs are special prescribed points, and this was verified by the observation that the footpoints do not move in this type of CME.

The other type of CME is the 'bubble-type', which is associated with the flare blast from explosive flares. We confirmed the association of this type of CME with the so-called EIT (Extreme Ultra-violet Imaging Telescope) waves, but the velocity of expansion of the bubble is twice or more greater than that of the EIT waves depending on events. Although EIT waves were widely considered to be Moreton waves viewed by SoHO/EIT in the solar activity minimum period, recent simultaneous observations of both have revealed that the EIT wave is something different from the Moreton wave, and propagates separately with a velocity less than half that of a Moreton wave. We therefore propose a new overall picture: the bubble-type CMEs are the flare-produced MHD blast waves themselves, whose skirt is identified as a Moreton wave. EIT waves may be interpreted as follows: the slow-mode gas motions from the source cause secondary long wavelength fast-mode waves which are trapped in the "waveguide" in the low corona. The secondary long-wavelength wave in the fast-mode, which is trapped in the low corona, has a slower propagation velocity due to the nature of the waves trapped in a "waveguide". This trapped wave induces slow-mode motions of the gas through a mode-coupling process in the high chromosphere, where the propagation velocities of the fast- and slow-mode waves match.

Three-dimensional MHD simulations for these two types of CME are in progress, and are previewed in this paper.

Keyword: Sun: coronal mass ejections

1 Introduction

It has been claimed that there are two types of CME with and without acceleration (Sheeley 1999), but some researchers (e.g. R. Schwenn 1997, private communication) seem to claim that all CMEs are of the bubble-type which was first discovered by Howard et al. (1979) as a halo CME (a bubble-type CME directed towards the Earth). There seems to be little consensus on whether or not there are two types of CME at present.

Here, we would like to present our results, which indicate that there are two types of CME in the SoHO/LASCO data. This supports Sheeley's (1999) view. However, we provide some physical arguments in relation to the two types. We first describe the observational basis for our arguments, and then give some explanation of our models for these two types (now in preparation in fuller forms with 3D MHD simulations by J. Kuwabara, R. Cameron, & Y. Uchida; R. Cameron & Y. Uchida; R. Cameron, Y. Uchida, & M. Nakamura).

The two types that we are claiming exist are (1) loop-type, and (2) bubble-type. The loop-type has the shape of a large loop with two fixed footpoints (often one in the northern and the other in the southern hemisphere). This type is associated with an arcade flare occurring somewhere between (or close to one of) the footpoints. The expansion accelerates as the CME rises, but may well saturate in velocity at greater distances. The bubble-type has the shape of a bubble, expanding with roughly constant speed, associated with explosive flares and with EIT waves. It is not natural to associate this bubble-shaped structure with the two clearly defined legs that keep connections to the photosphere in the case of the loop-type CMEs. The ratio of enhancement of the density over that of the normal corona is 20% or so for loop-type CMEs while only a few per cent for bubble-type CMEs (Hata 2001).

Naturally, there may be cases in which both types coexist in one and the same event because there are some arcade type flares which have an explosive component in them. However, we deal with pure and clear cases of each type in the following, in order to see the essential aspects more clearly.

We use data from SoHO/LASCO, SoHO/EIT, and Yohkoh, and report our preliminary results first.

2 Loop-type CMEs

We first concentrate on the loop-type CMEs. These are characterised by their loop-like shape with fixed footpoints. They typically have 20% or so enhancement in

 10.1071/AS01043 1323-3580/01/04345$05.00

density, accelerate as they expand outwards to a certain height, and deform their shape during the expansion in very characteristic ways in some cases.

2.1 Fixed Footpoints, and Their Relation to the Arcade Flare between Them

We first examined whether the footpoints of CMEs move during the event or not, and found that there are CMEs whose footpoints do NOT move. We specifically examined footpoint movement because previous satellites (Skylab, SMM, etc.) found that there was no substantial motion of CME footpoints. So our finding that there are CMEs whose footpoints stay fixed is a confirmation of the results from previous satellites (Hundhausen 1993). An example of this type is shown in Figure 1. It is seen that the loop structure has fixed footpoints, and the higher part of the loop deforms in a very characteristic way.

For this event, we performed a deep survey of faint structures in the pre-event phase, using Yohkoh soft X-ray images a few days before the event. It was found, in the in-depth examination by Tanaka (2000), that there existed faint connections between the locations of the footpoints of the CME and of the arcade flare. It is quite an important finding that the footpoints of CME are fixed at certain *prescribed* points that were connected with the region where the arcade flare occurs in the pre-event phase.

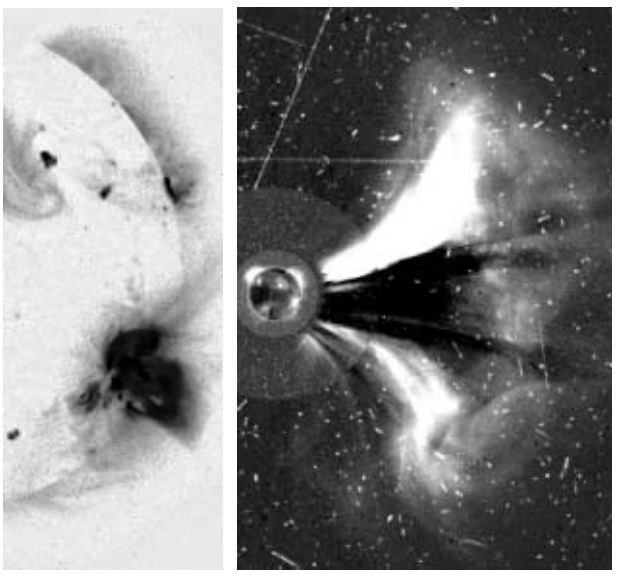

Figure 1 CME on November 6, 1997 (from Uchida 2000). The images are obtained by SoHO/LASCO C2 Camera for the event (b: right), and by deep-survey of Yohkoh/SXT image sometime before the event (a: left) (Tanaka 2000). The footpoints are fixed as seen in (b), and it was confirmed that there are connections between the location of the flare and the locations of the footpoints in the pre-event phase as seen in (a). In (b), it is seen that the high part of the loop starts deforming in the expansion. This shape is suggestive of a 3D shape of the loop, in which the high part probably flings away from the observer, just corresponding to the (transient) helical instability of the loop with the injection of torsional Alfvén wave packets (TAWPs) with opposite senses from each footpoint (J. Kuwabara et al., in preparation) (see Section 2.3).

The association of a flare which is seemingly isolated between the CME footpoints previously posed a riddle (Harrison & Sime 1989) — but the location where the flare occurred was actually magnetically connected to the future footpoints of the CME!

2.2 CMEs with the Second Loop Having a Dip in the Middle where the Associated Arcade Flare Exists

An example of a sub-type of loop-type CMEs with the fixed footpoints is shown in Figure 2. Such sub-types having dual loops may correspond to the CMEs described from the data of previous satellites (e.g. Hundhausen 1993). These structures are a frontal loop and a dark cavity between this and the second loop which is likely to be related to the rising dark filament hung in the middle. It is remarkable that the second structure clearly has a dip in the middle, and the location of the dip is right above the arcade flare between the footpoints (Figure 2, Yohkoh insert). A model of arcade flare and X-ray arcade formation considering quadruple magnetic sources (Uchida et al. 1999b; Hirose et al. 2001), which has increasing support from observations (Uchida et al. 1999c; Morita et al. 2001), is naturally compatible with this by forming a hexapole magnetic source situation (Uchida et al. 1999b; Uchida 2000).

2.3 Our Proposed Model for the Loop-type CMEs

Our interpretation (J. Kuwabara et al., in preparation) is that the first expanding structure is the compressed magnetic structure overlying the second structure which seems

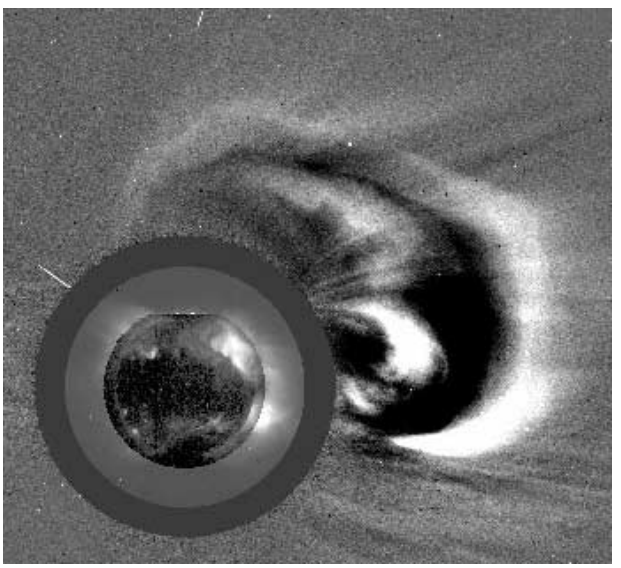

Figure 2 An example (from Uchida (2000)) of another sub-type of the loop-type CME, on December 6, 1997, in which the footpoints do not move, and the second loop showing a dip at the centre is following the first front (Tanaka 2000). The dip exactly corresponds to the location where the associated arcade flare occurred, suggesting that the dip is the anchored point released in the reconnection process in the flaring.

to be a structure whose central anchoring point is released by the flare between the footpoints. The first front may have a shape of a *paraglider wing*, but is likely to be different from the bubble shape of the bubble-type CMEs to be discussed in Section 3. Two pre-existing loops connecting the footpoints to the flaring site may become joined through reconnection in the flare, and form one long loop in this process (or, alternatively, it might be considered that a single pre-existing long loop held down by the magnetic fields in the active region is released), and rising with the dark filament in the dipped part. This single large loop whose middle point is released from the flare site will rise, gradually straightening itself and losing its dipped shape (Figure 2). With an injection from the flare site of a toroidal field into each of the two loops connecting the flare and the footpoints, the rising large loop is accelerated by the push given by the propagating torsional Alfvén wave packets (TAWPs), which may be released from the flare, and bounce from both footpoints back into the reconnected large loop. A helical instability of this large loop may occur when the amount of the toroidal field exceeds and violates the criterion for helical instability of the loop (corresponding to the Kruscal-Shafranov criterion for a similar but simpler straight geometry of a twisted flux tube).

Acceleration of the rising loop will be aided by magnetic buoyancy due to the magnetic field intensity gradient in the low corona. This acts on a magnetic structure, which is effectively dis-anchored from the solar surface. The magnitude of the energy available by this corresponds to the energy necessary to push such a structure into the region of stronger magnetic pressure. This is the 'melon-seed effect' discussed by Schlueter et al. (1958). It is possible that when a strong magnetic twist (TAWP) is injected from the flaring region and drives the loop rise by the TAWP's driving action, the expansion of the second structure may catch up with the first-going front, and may dominate in density and speed over the first one, and the CMEs may look, in some cases, like a single structure at a glance as in Figure 1.

3 Bubble-type CMEs Associated with Flare Blast Waves

3.1 Halo-type CMEs — A Bubble-type Coming Towards the Earth

The halo-type CME first found by Howard et al. (1979), expanding around the occulter of the coronagraph in all directions, is most likely to be a bubble-type front that is expanding toward the Earth, seen head-on. We therefore consider a bubble-like structure expanding into the interplanetary space from the Sun. An example is shown in Figure 3.

3.2 Relation of the Bubble-type CME to EIT Waves and Moreton Waves

Such bubble-like objects may be most naturally associated with expanding fronts seen to propagate on the solar surface with a circular (in many cases imperfectly circular) front. Moreton waves, which are seen as a front sweeping the top of the chromosphere with velocity 800–1500 km s^{-1}, were first found by Moreton (1961). This type of disturbance was given interpretation by one of the present authors as a sweeping skirt of an MHD blast wavefront propagating in the corona (Uchida 1968; 1970; Uchida, Altschuler, & Newkirk 1973), and the coronal part of the blast wave was considered to cause flare-related type II radio bursts when focused into the low-Alfvén velocity part of the corona and strengthened (Uchida 1974).

Thompson et al. (1998) discovered a front with SoHO/EIT, seen to propagate at 300–500 km s^{-1} in the EUV. This roughly circular front leaves behind it a (roughly) circular dark region surrounding the source. The circular front is called the EIT wave. The gas enhancing the intensity of emission in this wave is likely to be in the low corona, in contrast to the front of a Moreton wave which is detected in the Doppler shifted Hα-wing emitted from the high part of the geometrically thin chromosphere.

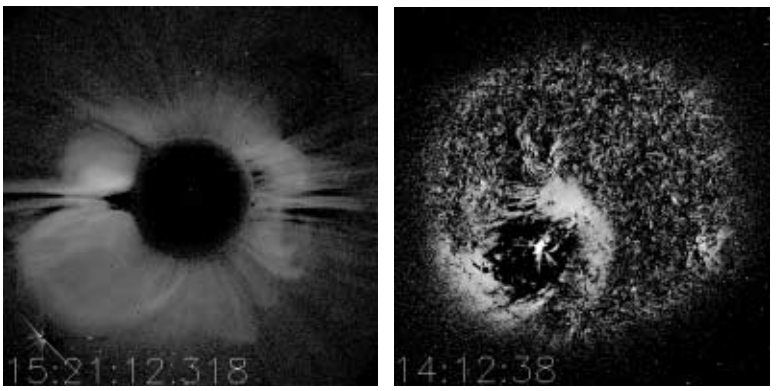

Figure 3 Association of a bubble-type CME with an EIT wave on April 7, 1999. Images for the CME (left) and EIT wave (right) (naturally at different times) are shown side by side (Hata 2001). It is seen clearly that both have the same origin, but the velocity of the bubble-type CME is twice or more faster than that of the EIT wave as shown in Figure 4.

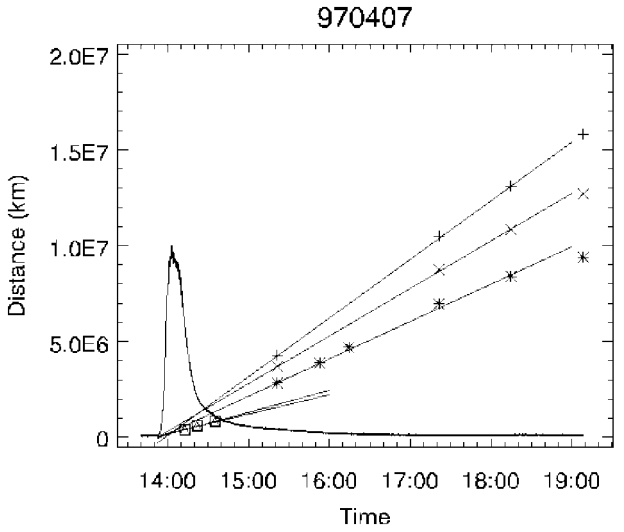

Figure 4 Distance versus time from the explosive flare of the fronts of the EIT wave and the bubble-type CMEs of Figure 3 in several directions (Hata 2001). The origins of both coincide in time with the flare start if we extrapolate those time–distance curves (lines) back in time. Note that the short lines correspond to the EIT wave data (limited to the solar disk) whereas the longer lines represent the bubble-type CME data.

The propagation velocity of an EIT wave, however, is considerably lower, but it has been widely considered that an EIT wave may be a Moreton wave seen in the EUV. The slower velocity of the EIT wave was considered to be due to weaker magnetic field strength during the activity minimum period.

Simultaneous observation of Moreton waves has not been performed until very recently, and therefore we began to study the relation of the bubble-type CMEs with EIT waves.

3.2.1 Association of Bubble-type CMEs with EIT Waves

Hata (2001) analysed the relationship between the halo-type CME and EIT wave caused by the same flare. He measured the velocities of propagation of the EIT wave and of the halo-type CME from a given explosive flare. An example of such analysis is given in Figures 3 and 4. Hata analysed the data of the EIT wave and halo-type CME in the form of a movie, but here, naturally, only typical frames are shown.

Figure 4 shows the time–distance diagram derived by analysing the time sequence. The curvature effect along the solar surface is corrected for the velocity of the EIT wave, whereas the velocity of the CME is measured as the velocity with which the greatest radius of the projected spherical front expands. The velocities of both are measured for several directions from the explosive flare.

The conclusions from the analysis of five events (Hata 2001) were: (i) the velocities of both are roughly proportional to each other for respective directions, (ii) the velocity of the EIT wave front is of the order of 300–500 km s^{-1}, and (iii) the approximately constant velocity of the bubble-type CME is of the order of 800–1100 km s^{-1}, roughly twice or more that of the EIT wave. The difference between these velocities is clear.

3.2.2 Discovery that the EIT Wave and Moreton Wave Are Different by Simultaneous Observations

EIT waves have been considered to be Moreton waves seen in EUV wavelengths. But the interrelation between Moreton waves and EIT waves was not clear because there were no simultaneous observations of Moreton waves until recently: the smaller velocity of the EIT wave could be explained as due to the weaker magnetic field strength in the activity minimum phase. The other explanation of the different velocity was that EIT waves and Moreton waves are different. Without simultaneous observations it was not possible to decide between these two possibilities until recently.

As soon as new observations of Moreton waves were made, and compared with EIT waves from the same flare event (Thompson et al. 2000; Eto et al. 2001), it became clear that these two are different because these two waves propagate as clearly separate fronts with different velocities: Moreton waves propagate with a velocity 'roughly twice or more' that of an EIT wave (note that also a separate sharper and less pronounced EUV disturbance, which is different from the slowly propagating diffuse 'EIT waves', was found as described in Thompson et al. (2000), corresponding to the Moreton wave front).

Therefore, together with the result (ii) in Section 3.2.1, we see that the bubble-type CMEs should be more naturally associated with Moreton waves, rather than with EIT waves.

3.3 Our Proposed Model for Disturbances from Explosive Flares — 3D MHD Simulations

3.3.1 Overall View

Our proposed interpretations of the flare-blast related phenomena are as follows:

1. The fainter and more frequent type of CME, which we call the bubble-type CME, will be explained as an extension of the flare blast wave due to an explosive flare. An MHD fast-mode front propagating out from the inner corona, weakening in intensity as it expands, gains strength again as it comes to the rarefied outer corona, and begins to blow away the low density gas there. There may be weak magnetic flux tubes being carried passively in this blowing out process, as are sometimes seen in the LASCO images, but these loops are passively carried and different from the actively expanding loop-type CMEs described in Section 2.

   That the bubble-type CMEs do not show marked acceleration or deceleration may correspond to the fact that the Alfvén velocity in the outer corona is slowly decreasing, but the strength of the shock slowly increases as the front moves into the increasingly rarefied corona.

2. Our interpretation of the Moreton wave is just as before: the blast wavefront in the MHD fast-mode propagates with a high speed in the corona, and the skirt of this blast wave sweeps the top of the chromosphere with a velocity of around 10^3 km s^{-1} (Uchida 1968; 1974; Uchida et al. 1973).[1]
3. What requires a new interpretation is thus EIT waves: in Uchida's approach using the eiconal equation (using a generalised WKB approximation with waves having wavelengths shorter than the scale lengths of quantities, and with $\beta \ll 1$), the behaviour of slow-mode waves, mode conversion, resonances, and dispersion did not come into the treatment due to approximations, and he concentrated on the sharp fast-mode pulse. We are now performing fuller 3D MHD simulations (R. Cameron et al., in preparation) for the situation in which effects left out before are included. We give in the following an overview of our results of the EIT wave model based on the more general treatment in simulations with the finite-difference method.

3.3.2 Trapping of Long Waves in the "Duct", and Coupling of Fast- and Slow-modes

To understand the EIT wave, the effect of long waves, whose wavelength is comparable to or greater than the scale length in the distributions of various quantities, as well as the coupling between the fast- and slow-mode waves, must be taken into account. These were not taken into account in the treatment of Moreton waves by Uchida due to the nature of the approximations adopted, as mentioned above.

R. Cameron et al. (in preparation) treated full 3D MHD simulations of this MHD blast wave behaviour in our MHD simulation scheme, and have shown that there indeed occurs a secondary more diffuse 'wavefront' propagating with roughly half the speed behind the first-going front! The simulation is a fully 3D MHD simulation using a finite difference scheme: the 3D MHD code, which is developed in our group for problems ranging from astrophysical jets (Uchida et al. 1999d; Nakamura, Uchida, & Hirose 2001) to that of solar flare problems (Hirose et al. 2001) and verified well, is used here.

Figure 5 shows a result of a 2.5D simulation, performed to elucidate the phenomena seen in 3D simulations, and shows that the solution has a first-going spherical front — the fast-mode wavefront corresponding to a sudden pressure rise (explosion) in the source — whose skirt sweeps through the chromosphere with a high velocity just as in Uchida's previous treatments, and later will start blowing out mass as it propagates into the rarefied outer corona.

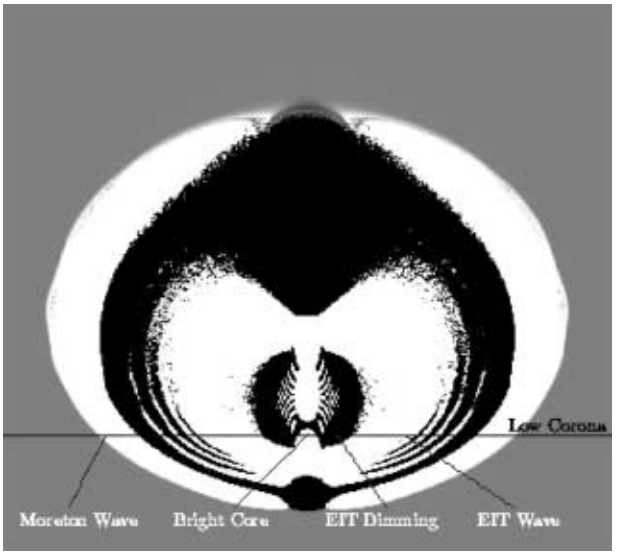

Figure 5 The result of 2D MHD simulation (R. Cameron & Y. Uchida, in preparation). The white part is high in gas pressure, and the black is low, and the grey is neutral. It is seen that there is first-going spherical blast wavefront propagating isotropically, with its skirt sweeping the top of the chromosphere just as in the model treated by Uchida (1968) by using the eiconal method. In the present treatment dealing with fuller processes, we see a wider second front propagating after the first.

We next note in the neighbourhood of the source that the material moves along the magnetic field (vertical here) both upwards and downwards. Such a mass motion rising from the source region is actually noted in the observations. These gas motions produce low-frequency long waves in the fast-mode like boatwaves. A long wave whose wavelength is comparable with the scale height can be trapped in the "wave duct" in the low corona. The propagation velocity in the waveguide becomes slower than that in the open space. This low-frequency long wave couples effectively with the slow-mode again at the high chromospheric part of the atmosphere in which the fast-mode and slow-mode propagation velocities (as well as that of the gravitational waves) are about equal to each other, and a resonance-like process may occur to supply the gas of the high chromosphere into the low corona (Hollweg 1979). Detailed elaboration of 3D MHD simulations, and elucidation by using 2D simulations, will be given in subsequent papers by R. Cameron & Y. Uchida, and R. Cameron et al. (in preparation), respectively.

4 Discussion

The frequency of occurrence of the bubble-type CMEs is expected to be much higher than that of the loop-type CMEs, because small explosive flares are much more frequent than large arcade flares, and even large arcade flarings (arcade flares near active regions, and arcade formations distant from active regions — both of these are

[1] Here, it is worth mentioning that Wang (2000) recently derived a result which is not in conformity with these, that the propagation velocity of the wavefront in the 'realistic condition' turned out to be low, and the rays are refracted upwards. In our preliminary view, his treatment with the locally 'realistic' field derived from the local photospheric magnetogram *left out* the effect of the weaker large scale magnetic sources at large distances, namely, the effect of the large scale sources like the global dipole, which is most important in the middle to high corona.

related to the loop-type CMEs) can have an explosive component in them.

All explosive flares of appreciable strength can be expected to produce fast-mode fronts of some magnitude, whereas only large arcade flares are likely to produce loop-type CMEs. The excess intensity of the bubble-type CMEs is lower than the loop-type CMEs by an order of magnitude (Hata 2001), and therefore may not have been very apparent with previous satellites, but the higher sensitivity SoHO/LASCO seems to have allowed the detection of numerous fainter bubble-type CMEs. Presumably more bubble-type CMEs would be detectable with even more sensitive instruments. In this circumstance, a first impression could be that all CMEs are of the bubble-type. But in view of the clear evidence for the existence of CMEs with fixed footpoints (supporting the results from previous satellites (Hundhausen 1993)), we can say that not all CMEs are of the bubble-type, though the bubble-type CMEs are certainly the most numerous. The loop-type CMEs are indeed fewer in number, but very clear examples, having loop shapes with fixed footpoints have actually been evidenced. They are denser and morphologically clearly different from the bubble-type CMEs.

Acknowledgements

We acknowledge T. Miyagoshi, T. Yabiku, S. Cable, S. Hirose, M. Nakamura, S. Uemura, and S. Morita for providing help in the series of works to be published in the CME connection. R. Cameron acknowledges the support by the Japan Society for the Promotion of Science Fellowship Program during his stay at the Science University of Tokyo.

References

Eto, S., et al. 2001, to be submitted to PASJ
Harrison, R. A., & Sime, D. G. 1989, J. Geophys. Res., 94, 2333
Hata, M. 2001, Master's Dissertation at Science University of Tokyo (in Japanese)
Hirose, S., Uchida, Y., Uemura, S., & Yamaguchi, T. 2001, ApJ, 551, 586
Hollweg, J. 1979, Solar Phys., 62, 227
Howard, R., et al. 1979, ApJ, 228, L45
Hundhausen, A. 1993, J. Geophys. Res., 98, 13177
Moreton, G. F. 1961, Sky and Telescope, 21, 145
Morita, S., Uchida, Y., Hirose, S., Uemura, S., & Yamaguchi, T. 2001, Solar Phys., 200, 137
Nakamura, M., Uchida, Y., & Hirose, S. 2001, New Astronomy, 6, 61
Schlueter, A. 1958, in Electromagnetic Phenomena in Cosmic Physics, ed. Lehnert (Cambridge: Cambridge University Press), 71
Sheeley, N. 1999, J. Geophys. Res., 104, 24739
Tanaka, T. 2000, Master's Dissertation at Science University of Tokyo (in Japanese)
Thompson, B., et al. 1998, J. Geophys. Res., 25, 246
Thompson, B., et al. 2000, Solar Phys., 193, 161
Uchida, Y. 1968, Solar Phys., 4, 30
Uchida, Y. 1970, PASJ, 22, 341
Uchida, Y. 1974, Solar Phys., 39, 431
Uchida, Y. 2000, in Advances in Solar Research at Eclipses from Ground and from Space, eds. J.-P. Zahn, & M. Stavinschi (Kluwer), 105
Uchida, Y., Altschuler, M. D., & Newkirk, G. 1973, Solar Phys., 28, 495
Uchida, Y., et al. 1999a, Astrophys. Space Sci., 264, 145
Uchida, Y., Hirose, S., Cable, S., Morita, S., Torii, M., Uemura, S., Yamaguchi, T. 1999b, PASJ, 51, 553
Uchida, Y., et al. 1999c, PASJ, 51, 53
Uchida, Y., et al. 1999d, in Highly Energetic Physical Processes and Mechanisms of Emission from Astrophysical Plasmas, eds P. Martens, S. Tsuruta, M. Weber, (San Francisco: ASP), 213
Wang, Y.-M. 2000, ApJ, 543, L89